Dynamical Complexities of Forced Impacting Systems

S. Foale and S. R. Bishop

Email alerting service   Receive free email alerts when new articles cite this article - sign up in the box at the top right-hand corner of the article or click **here**

Dynamical complexities of forced impacting systems

By S. Foale and S. R. Bishop

*Centre for Nonlinear Dynamics and its Applications, Civil Engineering Building,
University College London, Gower Street, London WC1E 6BT, U.K.*

The model of a forced linear oscillator with instantaneous impacts at one or two stops is discussed. The nonlinearities introduced by the instantaneous impact rule are sufficient to cause typical nonlinear behaviour. The impact rule is discontinuous, introducing discontinuities into discrete time Poincaré maps defined from the continuous time dynamical system. Discontinuities also exist in the derivatives of these maps. The implications of these discontinuities are discussed and their relevance to engineering applications is assessed with suggestions for further research.

---

1. Introduction

Periodically forced systems with impacts at rigid stops on one or two sides are commonly encountered in engineering. Examples include forced mechanical systems with clearances such as rattling gears (Pfeiffer 1990), impact printer heads (Tung & Shaw 1988), heat exchanger tubes subject to aerodynamic excitation (Whiston 1987) and vibration absorbers (Sharif-Bakhtiar & Shaw 1988), as well as examples from marine engineering such as the articulated mooring tower (Thompson *et al.* 1984), ships moored against fenders (Lean 1972) and the interaction between a sleeve and pile in the installation of a jacket structure over a pre-drilled template (Robinson & Ramzan 1988).

In engineering, systems are mathematically modelled using Newton's laws of motion and the model is investigated to identify, and thus avoid, unacceptable responses of the system. In the case of impacting systems this will usually involve parametric studies to identify regions with high velocity impacts which cause the greatest wear or damage, for example Nguyen *et al.* (1986). Parametric studies for the articulated mooring tower by Thompson *et al.* (1983) for a one sided impacting system show many resonant peaks, harmonic and subharmonic. It is also important to identify parameter values where a 'safe' solution disappears at a bifurcation leading to a jump to a distant, possibly unacceptable solution. It may also be desirable to locate regions where chaotic solutions exist so as to avoid the irregular nature of the resulting motion. Shaw (1985*b*) showed the existence of chaotic motions in the two sided linear impact oscillator and Whiston (1987*b*) studied such motions in some detail for particular 'generic' classes of one sided and preloaded systems.

The collision with a stop can be viewed as a severe form of nonlinearity at the point (or in the region) of the impact. Theoretical studies of impact oscillators have used a simple one-dimensional mathematical model of a particle attached to a linear spring subject to a coefficient of restitution rule at motion limiting stops. We shall

consider such an equation where the mass and stiffness have been scaled out leaving the four parameters: damping β, forcing amplitude α, forcing frequency ω and the coefficient of restitution r:

$$\begin{aligned}
\ddot{x} + 2\beta\dot{x} + x &= \alpha\cos\omega t, \quad b < x < a, \\
\dot{x} &\to -r\dot{x}, \quad x = a \quad \text{or} \quad x = b.
\end{aligned} \tag{1}$$

This equation is quite general, encompassing both one sided impacting as well as two sided by putting one of the stops at infinity (i.e. $a = \infty$ or $b = -\infty$.) Many previous studies of systems of this kind in the literature include only one mechanism for energy loss, either by setting the coefficient of restitution $r = 1$ or by putting the linear damping coefficient $\beta = 0$. The $\beta = 0$ case is not generic since motions which impact once will always impact again. Energy is always lost during impact in a real system due to both mechanisms, thus both are included here for completeness.

2. Methods of solution

The dynamical system (1) has the advantage of having at least partial analytical solutions. The differential equation can be solved completely given a set of initial conditions. Two constants of integration are obtained from the initial conditions which completely define the evolution of the system until a stop is encountered (i.e. $x = a$ or $x = b$). The coefficient of restitution rule $\dot{x} \to -r\dot{x}$ is then applied, which gives a new set of initial conditions and therefore a new equation defining the evolution of the system. The existence of such partial solutions allows some particular solutions of the system to be found analytically. Extensive use of this fact has been made in the literature (for example Shaw 1985a; Shaw & Holmes 1983; Whiston 1987a; Hindmarsh & Jefferies 1984) to locate harmonic and subharmonic solutions undergoing low numbers of impacts together with their stability. There is, however, only a limited amount of information which can be obtained in this way alone since the algebra soon becomes unmanageable for high numbers of impacts.

The existence of partial analytical solutions simplifies the numerical investigation of the system. No approximate integration routine need be used, since the partial solutions can be used in conjunction with some root finding method to locate the time when impacts occur very precisely. New constants of integration are then calculated after the impact rule has been applied and the next time when an impact will occur is located. In this way numerical errors can be kept very small.

3. Definition of Poincaré mappings

The three dimensional phase space of system (1) defined by $(x, \dot{x}, \phi)$ is portrayed in figure 1a as a box with the two ends at $\phi = 0$ and $\phi = T$ identified (where the phase ϕ is defined by $\phi = t \bmod T$, $T = 2\pi/\omega$). A stable orbit of the flow is represented by a dotted line in this figure. Another representation of this stable orbit in the phase plane projection is shown in figure 1b in which the orbit is projected down onto the displacement–velocity plane. The phase space box in figure 1a is bounded by the surfaces $\Sigma_{\mathrm{S}}, \Sigma_{\mathrm{L}}, \Sigma_{\mathrm{R}}$, where

$$\begin{aligned}
\Sigma_{\mathrm{S}} &= \{(\phi, x, \dot{x}), b \leqslant x \leqslant a, \phi = 0, -\infty < \dot{x} < \infty \\
\Sigma_{\mathrm{R}} &= \{(\phi, x, \dot{x}), x = a, 0 \leqslant \phi < T, -\infty < \dot{x} < \infty \\
\Sigma_{\mathrm{L}} &= \{(\phi, x, \dot{x}), x = b, 0 \leqslant \phi < T, -\infty < \dot{x} < \infty
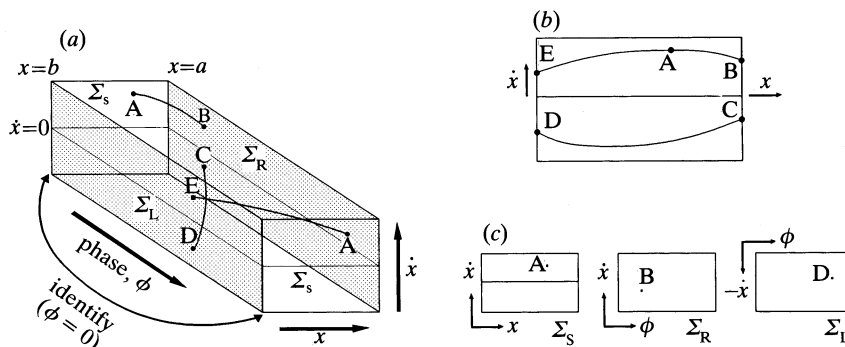\end{aligned} \tag{2}$$

Figure 1. (*a*) Three-dimensional phase portrait of double sided impacting system showing a stable orbit A–E, and (*b*) its phase plane projection. (*c*) The associated stroboscopic and right and left impact maps.

These surfaces are sections through the flow and form natural candidates for Poincaré sections which then define a two dimensional mapping from the three dimensional flow. The flow is followed from any point in a section Σ until it again intersects with that section Σ; this defines the mapping $P : \Sigma \to \Sigma$ (see Thompson & Stewart 1986 for more details). Three mappings are defined in this way: $P_{\mathrm{S}} : \Sigma_{\mathrm{S}} \to \Sigma_{\mathrm{S}}$, the stroboscopic map where the displacement and velocity are sampled at a given phase once every cycle of the forcing, and the two impact maps $P_{\mathrm{L}} : \Sigma_{\mathrm{L}-} \to \Sigma_{\mathrm{L}-}$ and $P_{\mathrm{R}} : \Sigma_{\mathrm{R}+} \to \Sigma_{\mathrm{R}+}$ where the phase and velocity are sampled at an impact. The subscripts $+$ and $-$ here denote that the sections are restricted to only positive or only negative velocities since impacts can only occur on the right stop with positive velocity and on the left with negative velocity. Note that the limit cycle sketched in figure 1*a* repeats after one forcing period (it is the same at $\phi = 0$ and $\phi = T$), i.e. it has period one. This leads to a stable fixed point existing under one iteration of the stroboscopic map Σ_{S}, represented by the dot A in figure 1*c*. The orbit impacts once at each stop before repeating, so there is also a stable fixed point under one iteration of each of the impact maps, represented by the dots at B and D in the diagrams in figure 1*c*. It is not necessary that a stable steady state which has a fixed point of order one under P_{S} should have a fixed point of order one under P_{L} or P_{R}. A period n limit cycle can impact p times at the left stop and q times at the right before repeating, where n, p and q are all different. It is not even necessary for impacts to take place on a particular stop at all: the stable state may involve repeated impacts on only one stop, or may not impact at either stop. This is a disadvantage of only considering impact maps: they do not necessarily capture information about all of the possible asymptotic steady states of a system. However, important physical information is conveyed by the impact map. A point on the impact map has as one of its coordinates the velocity at impact, which is a quantity which could relate to the amount of damage done to the system at the stops. Stroboscopic maps capture every asymptotic steady state, but there is no direct information in the position of the fixed point in this map as to the severity of the impacts.

4. Discontinuities of the mappings

The discontinuous nature of the impact rule and the choice of section leads to discontinuities in both types of mapping described above. Discontinuities arise in the
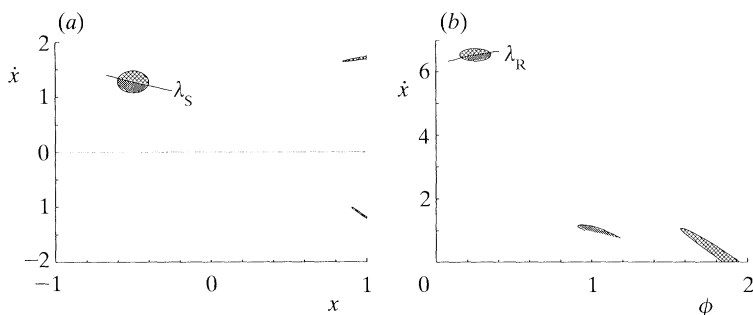
Figure 2. (a) Local area spanning the line mapping to the right-hand stop λ_s and its image under P_S. The top portion maps to the positive velocity area against the stop at $+1$, the bottom to the negative velocity area. (b) Area spanning the line mapping to zero velocity and its image under P_R. In both pictures $a = 1$, $b = -1$, $r = 0.7$, $\beta = 0.05$, $\omega = 1.9$, $\alpha = 2.7$.

stroboscopic map due to the impact itself. Consider a line of points λ_S in Σ_S which map to a stop in one period, i.e. λ_S is defined by

$$\lambda_S = \{x \mid x \in \Sigma_S, P_S(x) = (a, y), 0 < y < \infty\}. \tag{3}$$

Each point on this line will, due to the instantaneous reversal of velocity defined by the impact rule, map to two points (a, y, ϕ) and $(a, -ry, \phi)$. A small area which spans the line λ_S will map to two separate areas as shown in figure 2a. The two local portions of area either side of the line λ_S are shaded differently and then mapped forwards under one iteration of P_S to two disjoint areas which are shaded correspondingly. These areas are simply related along their borders at the stop, one being $-r$ times the other. This type of discontinuity, though not apparent in smooth dynamical systems, is merely an artefact introduced by the impact rule and is not 'serious'. A fixed point in the stroboscopic map which approaches a stop at $x = a$ in the positive half plane as a parameter is smoothly varied will 'reappear' in the negative half plane with $-r$ times the velocity and its position will then continue to move smoothly.

Impact mappings on the other hand have discontinuities of a more serious nature. Consider now the line λ_R in the impact section Σ_{R+} which maps to the zero velocity line, i.e.

$$\lambda_R = \{z \mid z \in \Sigma_{R+}, P_R(z) = (\phi, 0), 0 \leqslant \phi < T\}. \tag{4}$$

A point on one side of this line will map under P_R to a low velocity impacting point. On the other side of the line, the flow will just fail to impact and the next impact (if there is one at all) will be in a position quite unrelated by any simple rule. A small area spanning this line will map to two disjoint areas: one which has the zero velocity line as a boundary and one which is completely disconnected, as in figure 2b in which an ellipse placed around a section of λ_R is mapped forwards under P_R. Again, the two portions either side of the line are shaded differently and the ellipse maps under one iteration of P_R to two disjoint areas which are shaded correspondingly. As was remarked above, the impact section is such that not all motions will cross it, and the discontinuity exists for essentially this reason. It should be noted that the same type of section could be defined for any system at some artificial 'stop position', and exactly the same kinds of discontinuities would arise. It is important to be aware of the discontinuous nature of these maps in order to interpret results obtained using

them. For example, basins of attraction for stable solutions need not be connected if the map is discontinuous.

5. Grazing bifurcations

If part of an orbit of an impacting system is just touching a stop with zero velocity, then it is said to be a grazing orbit. The derivative of the associated Poincaré map at a point along a grazing orbit is not defined. In any Poincaré section defined through a flow there will be a line of points λ which, if followed along the flow, will touch a stop with zero velocity. In general, in taking a derivative with respect to some variable at a point along this line, the limit from the non-impacting side will differ from that taken from the impacting side, thus a unique limit cannot be defined. In fact, some of the elements of the jacobian (first differential) matrix of the mapping on the impacting side of λ depend inversely upon the velocity at impact (Nordmark 1991), so low-velocity impacts will lead to very large elements. This result is valid not just for the linear impact oscillator (1) but any oscillator with the coefficient of restitution rule applied at impact. Although the determinant of the jacobian always remains bounded, in fact less than one since the system is always dissipative, an eigenvalue will tend to infinity at grazing (if the limit is taken on the impacting side.) From this we conclude that if a stable limit cycle of an impacting system goes through grazing at any point on the orbit under a change in parameters, the stable orbit must vanish; either the orbit becomes unstable or disappears completely. In other words some kind of bifurcation must have occurred, although not one of the standard bifurcations which occur when an eigenvalue of the determinant of the jacobian of a map passes through the unit circle on the complex plane (Thompson & Stewart 1986). As was noted above, orbits with low-velocity impacts can have a very large eigenvalue. Thus a further complexity of impacting systems is that areas around the line λ in a map undergo a large amount of stretching in one direction, even without a fixed point crossing λ causing a grazing bifurcation.

Figures 3 and 4 show a simple illustration of this grazing phenomenon. The attracting solution of the system from an initial condition at $\alpha = 2$ may be followed for increasing α. The path of an attractor is numerically calculated, and in figure 3 we show the x coordinate of the stroboscopic Poincaré map defined by taking a section of constant phase with $a = 1$, $b = -1$, $r = 0.7$, $\beta = 0.05$, $\omega = 1.9$ (this represents a symmetrical, two sided impacting system). This is achieved by simply allowing the system to evolve until the map 'converges' (to some predetermined degree of accuracy) to a fixed point or series of points (i.e. a fixed point of a higher iterate of the map, or subharmonic). The parameter being varied, in this case amplitude α, is then altered slightly and the system is allowed to converge onto an attracting fixed point, using as an initial condition the last point calculated at the old parameter value. The newly calculated solution will be a continuation of the path of the previous point unless a bifurcation has occurred. After a bifurcation, the system will stabilize onto a different, possibly remote, attractor which then in turn is followed.

Figure 3 shows the x coordinate of the Poincaré point calculated as described above, whereas figure 4 shows the shape of the limit cycle at the points A to E marked in figure 3. Initially, the limit cycle corresponding to the period one fixed point ($\alpha < 2.5$) does not impact at all. It therefore 'knows' nothing (locally) about the existence of the stops at $x = \pm 1$. The eigenvalues of the fixed point are just the
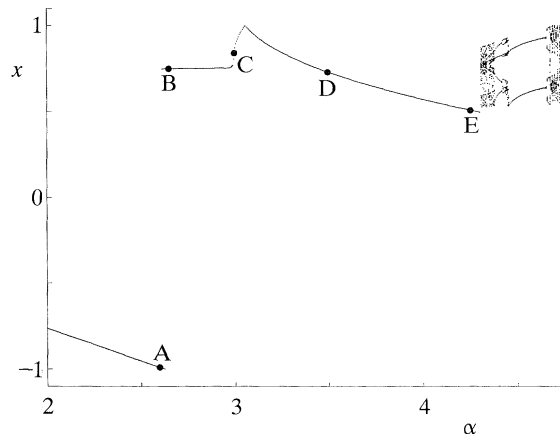
Figure 3. Path of x coordinate of attracting solutions in the stroboscopic Poincaré map as amplitude α increases, showing jumps in state at two grazing bifurcations. Other parameters as figure 2. Points A–E correspond to phase plane projections in figure 4.
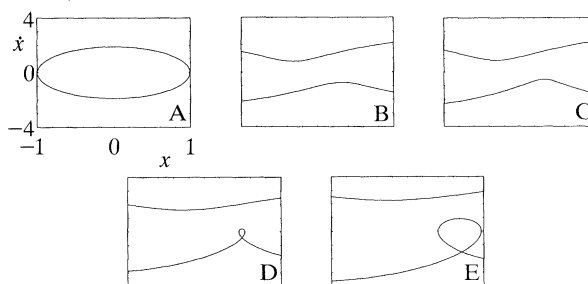

Figure 4. Stable orbits at: A, $\omega = 2.6$; B, $\omega = 2.65$; C, $\omega = 3.0$; D, $\omega = 3.5$; E, $\omega = 4.25$. Other parameters as figure 2. All figures have $-1 < x < 1$, $-4.0 < \dot{x} < 4.0$.

eigenvalues of the linear system. As the amplitude of the forcing, α, is increased to just over 2.5 this limit cycle goes through grazing. There is a sudden jump as the stable fixed point of the map loses its stability and the system falls onto the already existing period one solution. The orbit of the new attractor at B just after the bifurcation is shown in figure 4. This event looks like a saddle-node bifurcation and this observation will be addressed more fully in a forthcoming paper. However, up to grazing there is no local information to indicate that the jump is about to occur (an eigenvalue of the fixed point does not move smoothly towards the unit circle on the complex plane at $+1$). As α is further increased the symmetrical period one fixed point undergoes a symmetry breaking bifurcation just before C ($\alpha \approx 3$). With the symmetry broken, a loop develops on the projected orbit, as shown in figure 4 at D, which itself moves towards grazing at the right hand stop. As this orbit itself grazes at $\alpha \approx 4.3$ the stable period one fixed point disappears and there is an immediate transition to what appears to be a chaotic attractor (at least a long chaotic transient). The original order one stable fixed point has disappeared, the motion again falling on to an already existing solution, in this case apparently chaotic. Transition to this particular attractor is not as dramatic as in the case of a non-impacting attractor jumping to an impacting one. Maximum velocity at impact does increase (discontinuously), but only by a relatively small amount. This chaotic motion could even be viewed as less severe than the periodic solution since many
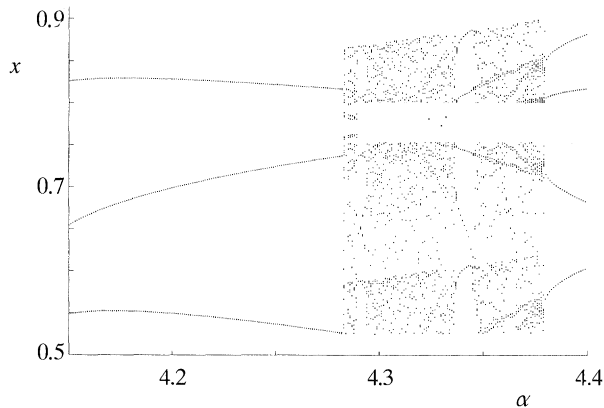
Figure 5. Enlargement of an area of the parametric study shown in figure 3 of response x showing the bifurcation from a period three attracting solution to chaos close to $\alpha = 4.3$.
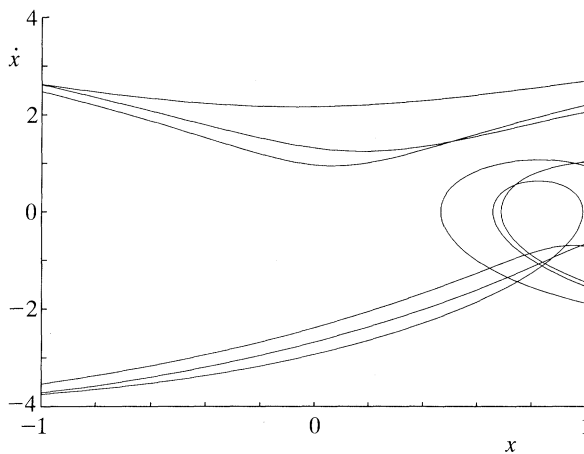

Figure 6. Phase projection of period three attracting solution onto displacement–velocity plane just before grazing bifurcation leading to chaos. Here $\alpha = 4.28$.

impact events will occur with a reduced velocity as well as some with greater velocity.

A further point of interest can be obtained by following for decreasing α the chaotic attracting solution from $\alpha \approx 4.3$. This path, shown in figure 5, is followed back until the chaotic attractor disappears at $\alpha \approx 4.28$, where the motion falls on to a period three limit cycle. Conversely, for increasing α, part of the loop of a period three limit cycle grazes (see figure 6) and a chaotic attractor is created at this bifurcation. Hence, if the path is followed for increasing or decreasing α the result is the same, with no hysteresis.

Three events that have been described as grazing bifurcations have been shown above. The simplest, and in terms of the potential for damage at the stops, the most dangerous, occurs when the non-impacting limit cycle grazes the stops and suddenly falls onto a coexisting impacting attracting solution. The other two grazing events appear to be similar just by examining the path following diagrams. A stable periodic orbit in both cases is seen to disappear at grazing to leave the motion exhibiting chaotic type behaviour. However, the grazing of the period one fixed point at $\alpha \approx 4.3$ is hysteric: a different path is followed for increasing and decreasing α. The chaotic
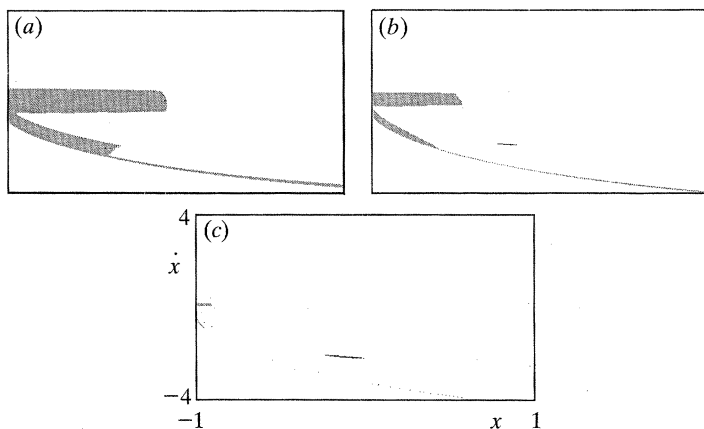
Figure 7. Basins of attraction for competing fixed points of P_s, $a = 1$, $b = -1$, $r = 0.7$, $\beta = 0.05$, $\omega = 1.9$, (a) $\alpha = 1.5$, (b) $\alpha = 2.0$, (c) $\alpha = 2.5$. All figures show the area $-1 < x < 1$, $-4.0 < \dot{x} < 4.0$, discretized into 640×350 cells. The shaded area represents starts resulting in non-impacting period one fixed point. The white area represents starts resulting in impacting fixed point.

attractor cannot be said to have been created at the grazing, since it exists at both higher and lower values of α, unlike the creation of chaos from the period three solution.

6. Global consequences of grazing

Locally the stability of an orbit is not affected by the approach to grazing and subsequent loss of stability as a parameter is varied. When studying the dynamics of a system it is important to know not only the locations and types of solutions present, but also how the basins of attraction for the various stable steady states are organized. In a real engineering system the size of the basin for a particular, safe solution should be large enough such that the inevitable noise present in any physical system does not cause a jump into the basin of a different possibly unsafe solution. Figure 7a–c shows the computed basins of attraction at a series of amplitude values leading up to the first grazing bifurcation from a non-impacting to an impacting motion. These diagrams were produced using a variant of Hsu's simple cell-to-cell mapping algorithm (Hsu 1985; Foale & Thompson 1991). The shaded basin in each case represents those starts which lead to the non-impacting period one solution, whereas the area left blank represents those starts which lead to the period one solution impacting once on either side. Clearly, although locally the non-impacting fixed point is perfectly stable in a mathematical sense, its basin shrinks and has virtually disappeared as grazing is approached, illustrated in figure 7c. Thus a small amount of noise in the system may well kick this fixed point out of its basin onto the impacting motion. A random start has very little chance of ending up on the non-impacting solution. Note that until the shaded basin finally disappears completely at the grazing bifurcation, the area of this basin must be infinite due to the dissipative nature of the map. A wispy grey 'tail' can be picked out even in the figure 7c. Any apparent breaks in the tail are only a result of numerical discretization errors (where the basin is thinner than one cell). The small black areas in each of figure 7a–c represent the basin of attraction of a motion which impacts an infinite number of times (with decreasing velocities to come to rest at a stop) before leaving the stop again.

7. Discussion

It has been shown that introducing a nonlinearity into a linear oscillator by using an instantaneous impact rule can result in complicated behaviour. Not only does the system of type (1) exhibit behaviour that typically occurs in smooth nonlinear systems, but there are additional complexities and non-typical behaviour which result from the way in which the impact is modelled. The discontinuities in both stroboscopic and impact mappings, though of mathematical interest, do not pose a practical problem. If a more realistic, continuous model for the impact process were used, for example a stiff spring, the area in figure 2*a* which maps to two disjoint areas touching the stop would map to two similar areas joined by a thin strip. The impact type map in this case would still have discontinuities, but these are due to the choice of a section which is not always transverse to the flow and not an inherent problem in the system.

Discontinuities in the derivative of Poincaré maps defined from impacting systems are the cause of the grazing bifurcation. Two distinct types of grazing bifurcation have been demonstrated in this paper: one in which the stable motion disappears and the system stabilizes onto an already existing attracting solution, the other in which there is an immediate jump to chaos as part of an orbit grazes at a stop. In both cases, as a result of the bifurcation, the system undergoes a rapid jump to motions with large amplitude.

The practical importance of the complexities arising in impacting models needs to be fully assessed. On the one hand it appears that the use of a continuous model overcomes some of these difficulties while physical systems are seen to undergo changes in their response resembling those seen in the simple model considered here (Robinson & Ramzan 1988). The need for further work is thus in identifying qualitative behaviour common to both discontinuous and smooth systems.

References

Foale, S. & Thompson, J. M. T. 1991 Geometrical concepts and computational techniques of nonlinear dynamics. *Comp. Meth. appl. Mech. Engng.* **89**, 381–394.

Hindmarsh, M. B. & Jefferies, D. J. 1984 On the motions of the offset oscillator. *Phys. A Math. Gen.* **17**, 1791–1803.

Hsu, C. S. 1987 *Cell-to-cell mapping: a method of global analysis for nonlinear systems.* New York: Springer.

Lean, G. H. 1971 Subharmonic motions of moored ships subjected to wave action. *Trans. R. Institute Naval Architects* **113**, 387–399.

Nguyen, D. T., Noah, S. T. & Kettleborough, C. F. 1986 Impact behaviour of an oscillator with limiting stops, part I: A parametric study. *J. Sound Vib.* **109**, 293–307.

Nordmark, A. B. 1991 Non-periodic motion caused by grazing incidence in an impact oscillator. *J. Sound Vib.* **145**, 279–297.

Pfeiffer, F. & Kunert, A. 1990 Rattling models from deterministic to stochastic processes. *Nonlinear Dynamics* **1**, 63–74.

Robinson, R. W. & Raman, F. A. 1988 Prediction of jacket to template docking forces during installation. Preprint.

Sharif-Bakhtiar, M. & Shaw, S. W. 1988 The dynamic response of a centrifugal pendulum vibration absorber with motion-limiting stops. *J. Sound Vib.* **126**, 221–235.

Shaw, S. W. & Holmes, P. J. 1983 A periodically forced piecewise linear oscillator. *J. Sound Vib.* **90**, 129–155.

Shaw, S. W. 1985*a* Dynamics of harmonically excited systems having rigid amplitude constraints, Part I – Subharmonic motions and local bifurcations. *J. appl. Mech.* **52**, 453–458.

Shaw, S. W. 1985*b* Dynamics of harmonically excited systems having rigid amplitude constraints, Part II – Chaotic motions and global bifurcations. *J. appl. Mech.* **52**, 459–464.

Thompson, J. M. T., Bokaian, A. R. & Ghaffari, R. 1984 Subharmonic and chaotic motions of compliant offshore structures and articulated mooring towers. *J. Energy Resources Technol.* **106**, 191–198.

Thompson, J. M. T. & Stewart, H. B. 1986 *Nonlinear dynamics and chaos.* Chichester: Wiley.

Tung, P. C. & Shaw, S. W. 1988 The dynamics of an impact print hammer. *J. Vib. Acoust. Stress Reliability Design* **110**, 193–200.

Whiston, G. S. 1987 The vibro impact response of a harmonically excited and preloaded one dimensional linear oscillator. *J. Sound Vib.* **115**, 303–319.

Whiston, G. S. 1987 Global dynamics of a vibro impacting linear oscillator. *J. Sound Vib.* **118**, 395–429.